

P.A.C.S. numbers:05.70.Fh, 64.60.Cn, 75.10.Hk, 75.10.Nr

Canonical local algorithms for spin systems: Heat Bath and Hasting's methods

D. Loison^{1*†}, C. Qin², K.D. Schotte¹ and X.F. Jin³

¹*Institut für Theoretische Physik, Freie Universität Berlin,
Arnimallee 14, 14195 Berlin, Germany*

²*Institute for Materials Research, Tohoku University, Sendai 980-8577, Japan*

³*Surface Physics Laboratory, Fudan University, Shanghai 200433, China*

Abstract

We introduce new fast canonical local algorithms for discrete and continuous spin systems. We show that for a broad selection of spin systems they compare favorably to the known ones except for the Ising ± 1 spins. The new procedures use discretization scheme and the necessary information have to be stored in computer memory before the simulation. The models for testing discrete spins are the Ising ± 1 , the general Ising S or Blume-Capel model, the Potts and the clock models. The continuous spins we examine are the $O(N)$ models, including the continuous Ising model ($N = 1$), the ϕ^4 Ising model ($N = 1$), the XY model ($N = 2$), the Heisenberg model ($N = 3$), the ϕ^4 Heisenberg model ($N = 3$), the $O(4)$ model with applications to the $SU(2)$ lattice gauge theory, and the general $O(N)$ vector spins with $N \geq 5$.

PACS numbers:

* corresponding author: Damien.Loison@physik.fu-berlin.de

† Work supported by Deutsche Forschungsgemeinschaft under Grant No. Scho158/10

I. INTRODUCTION

Spin systems are one of the most studied subjects in physics for their own interest but also because many other problems can be mapped on them. Since few exact calculations are available, numerical Monte Carlo simulations are extensively used to study them. One of the most popular method is the Metropolis algorithm[1], rightly because of its simplicity and its general applicability. The Metropolis algorithm is the easiest one to implement since it uses no prior informations and automatically matches the properties of the systems. However, using more of the available informations one should obtain algorithms better suited to spin systems. The algorithms proposed in this article follow this strategy at the price that they are slightly more complicated. To help implementations all programs discussed in this article are accessible at our homepage [2].

The algorithms studied in this article use only local updates. The non-local cluster algorithms are certainly better suited to study ferromagnetic second order phase transitions but cannot be used for frustrated spin systems and for first order transitions. Moreover, even when available, cluster algorithms should be used in combination with local algorithm [3]. The gain in efficiency quoted in the present article must be understood as the gain for the part corresponding to the local algorithm alone. Further we have checked the influence on the gain of other algorithms like the exchange algorithm[4], the over-relaxation algorithm [5] or the multicanonical algorithm [6]. We think that, if the multi-spins coding cannot be implemented, the methods introduced in this article are the fastest possible local updates and no real improvements could be made. If the multi-spins coding can be implemented it should be used because the gain will be better. However, this method is less general than the methods introduced in this article and moreover exist only for discrete spins.

Simulations to test the algorithms have been done for several lattices with frustrated or non frustrated spin systems, using small lattice sizes L . The examples studied are the two-dimensional ferromagnetic square lattice (2s), the two-dimensional antiferromagnetic triangular lattice (2t), the three-dimensional antiferromagnetic stacked triangular lattice (3t), the three-dimensional ferromagnetic and anti-ferromagnetic cubic lattice (3c & 3ca), and the four-dimensional spin glasses on a cubic lattice with random $\pm J$ interaction (4sg).

The comparative efficiency of the algorithm studied does not depend on the size, due to the local nature of the updates. For a second order transition the integrated autocorrelation

time (see for example the appendix of [7]) follows the same law $\tau = \tau_0 \cdot L^z$ with $z \approx 2$ and only the value of τ_0 depends on the algorithm used. In a strong first order transition τ has an exponential form for a local algorithm but the multicanonical algorithm in combination gives a power law behavior with a different z [6]. Also, because algorithms are local, the type of lattices and interactions do not have a strong influence on the comparative efficiency of the algorithms. The important parameter is the temperature or more precisely the local field, that is the sum of the neighboring spins associated with interactions divided by the temperature. Therefore the methods introduced are not restricted to the lattices studied here but will be applicable to other lattices as well.

Most of the algorithms proposed use arrays to store values calculated prior to the simulation. The performances of the programs depend therefore crucially on the access time to the memory and in particular on the size of cache memory. For the simulations an Athlon 1800 processor with 250 Kb cache memory has been used. This amount has quadrupled to 1 Mb with new processors now available (in 2004) and therefore the performances of the proposed algorithms should also increase. Moreover the performance also strongly depends on the compiler used. We used the Intel compiler “icc” with the optimization “-O” and obtained a code two times faster than the one with the “gcc” compiler.

In the following we start with a reexamination of the detailed balance condition. Then we introduce different algorithms trying them out on several types of discrete and continuous spins. The discrete spin systems we consider are the ± 1 Ising spin, the general Ising spin with $S > 2$ states, the Potts and the clock models. For the continuous spins we investigate continuous Ising spins $-1 \geq S \geq +1$, the Ising ϕ^4 -model, XY spins, Heisenberg spins, the Heisenberg ϕ^4 -model, and also the $O(N)$ spin models for $N \geq 4$.

II. DETAILED BALANCE CONDITION

The basis in the simulation techniques we are going to discuss is the detailed balance in the updating process[8]. There the essential point is symmetry in time: the probability $P(A)$ of an initial configuration A multiplied by the transition probability $T_{A \rightarrow B}$ to a new or final configuration B should be equal to the probability for the inverse process starting from the configuration B with $P(B)$ and transition probability $T_{B \rightarrow A}$, so that

$$P(A) \cdot T_{A \rightarrow B} = P(B) \cdot T_{B \rightarrow A} . \quad (1)$$

In choosing the transition probabilities T properly the spin configurations will be visited with the weights P and these are for a canonical system the Boltzmann weights. To be more flexible the detailed balance condition (1) should be rewritten in the form

$$\frac{P(A)}{f(B, A)} f(B, A) \cdot T_{A \rightarrow B} = \frac{P(B)}{f(A, B)} f(A, B) \cdot T_{B \rightarrow A} \quad (2)$$

with an auxiliary function f depending on the two states A and B . There are essentially two ways to satisfy these equations, the “heat bath” method and the “Hasting” method, this last one includes the Metropolis method.

In the first case the transition probability $T_{A \rightarrow B} = T(B)$ and the function $f(A, B) = f(B)$ depend only on the final state B , so that the detailed balance condition is reduced to

$$T_{A \rightarrow B} = P(B) = \frac{P(B)}{f(B)} \cdot f(B) . \quad (3)$$

The simplified form $T(B) = P(B)$ should be used if the probability can be integrated “easily” and inverted like for the discrete spins or Heisenberg spins. In principle any probability function $P(B)$ depending on one variable could be integrated and inverted numerically and the result stored in tables. However, this method is not recommended for spin systems like XY spins for example, since the tables become too large and the algorithm will be costly in computing time to get sufficiently small errors. For such a case it is better to use the second form of eq. (3) and proceed as follows.

The first procedure is the “heat bath” method. One finds a new configuration $B = F^{-1}(\text{ran})$ using a random number “ran” and the inverse of the function F which is the sum or the integral of f . Having found the new state B , it is accepted with the probability $\frac{P(B)}{f(B)}$ with a new random number $0 \leq \text{ran}_2 < 1$ by the usual rejection method if $\frac{P(B)}{f(B)} \geq \text{ran}_2$. The function $f(B)$ must be always larger than $P(B)$ but the difference should be small since otherwise too many choices for the new states will be rejected. The simplified case corresponds to $f(B) = P(B)$ and no second random number is needed.

The second procedure is Hasting’s method [9] with the transition probability equal to

$$T_{A \rightarrow B} = f(A, B) \cdot \min \left(\frac{P(B) \cdot f(B, A)}{P(A) \cdot f(A, B)}, 1 \right) . \quad (4)$$

Putting this into (2) it is not difficult to see that the detailed balance condition is indeed fulfilled. The function f can here be smaller or larger than P which is of advantage compared to the stricter condition for the heat bath method. If one chooses $f(A, B) = 1$ for any A and

B one gets the transition probability of the Metropolis method [1]. The gain in efficiency due to Hasting’s generalization can be quite large in comparison to the Metropolis update depending on the spin model, the choice of the function f and the temperature range of the simulation.

Whatever the method used will be, it should be ergodic, i.e. all configurations should be accessible. Since our special choices for the function f will be of a kind for which the local updates do not change in an essential way from the ones in use, we will not come back to this point. In the following we have to treat discrete and continuous spin systems separately.

III. DISCRETE MODEL

A. Simulation methods

We present in this section six algorithms we have implemented for discrete spins. We assume that the spins have q possible states $(1, 2, \dots, q)$. The actual or old state is A and the new state B as before.

1. Metropolis

The first method one tries usually is the Metropolis algorithm [1] abbreviated as Me in the figures. As discussed in the preceding section in eq. (4) the choice is $f(A, B) = 1$ whatever the states A, B are. The implementation is as follows:

1. Choose randomly one of q states B using $\text{int}(q \cdot \text{ran}_1)$ with ran_1 a random number in the range $0 \leq \text{ran}_1 < 1$ or in the interval $[0, 1[$. The function “int” gives the largest integer smaller than the floating point number.
2. Accept this new state with another random number, if $P(B)/P(A) > \text{ran}_2$.

There are two problems to be noted:

- a. The choice of the new state can be identical to the old one.
- b. The choice of a new state is equiprobable, but in particular at low temperatures the Boltzmann probabilities $P(B)$ will be quite different. This fact will lead to a large and unproductive rejection rate.

2. Restricted Metropolis

A way to solve the first problem is to choose the new state randomly omitting the actual state. We denote this as the restricted Metropolis algorithm or Me_δ . With the choice $f(A, B \neq A) = 1$ and $f(A, A) = 0$ eq. (4) is practically the same as for the Metropolis algorithm Me . The implementation is therefore:

1. Choose randomly one state B using $\text{int}((q-1) \cdot \text{ran}_1)$ and use a list to find randomly one of the $q-1$ states different from A .
2. Accept this new state if $P(B)/P(A) > \text{ran}_2$.

Since the actual state is no longer tested using Me_δ one gains compared to Me an amount $1/q$ in the updating process. If q is large, this difference becomes negligible. For the Ising two-states case only the opposite state is tested anyway. But as a standard for $q > 2$ it is not used, as far as we know, where also the performance is improved in a measurable way as we will show.

As to the second problem b described at the end of the previous section it will be addressed by the heat bath method discussed next. In addition a restricted heat bath will solve both problems a and b simultaneously.

3. Direct Heat Bath

In discrete system the number of states is finite and one can simply choose the function $f = P$ in eq. (3). We call it here Direct Heat Bath or abbreviated *DHB*. The implementation is simple:

1. Calculate the $Norm = P(0) + P(1) + \dots$.
2. Take a random number ran in the range $[0, 1[$.
3. If $\text{ran} < P(1)/Norm$, the new configuration is chosen as 1.
4. Else if $\text{ran} < (P(1) + P(2))/Norm$, the new configuration is chosen as 2.
5. and so forth ...

This algorithm has two flaws:

- a. The new state can be identical to the old one.
- b. If there are too many possible states, the algorithm becomes very slow.

The first problem is similar to the Metropolis algorithm but at least the new state is chosen among really accessible states according to their probability $P(B)$. Therefore the acceptance rate is 1.

This algorithm is always more efficient than the Metropolis algorithm Me and also the restricted Metropolis method Me_δ . Only for Ising spins $S = \pm 1$ the Me_δ method is more efficient than this heat bath method.

4. Direct Heat Bath with Walker's alias

To solve the problem of the inefficiency of the Heat Bath method for a larger number of states q we propose to use Walker's alias method [10]. Since this procedure was, to our knowledge, never used in spin simulations, it needs some explanations.

Walker's alias method handles in an economic way which new state to choose among the q possibilities. The probabilities $P(q)$ for a new state i are not piled up on top of each other to sum up to 1 as in the simple heat bath described before, but stored in q different boxes of equal height $1/q$. Walker's construction has in each box only one or two different probabilities. For an example with $q = 3$ see fig. 5(b). Before the simulation starts one must have calculated and stored the probabilities P_{limit}^i which divides each box i . The upper states in each box must also be stored in an array. These states as "subtenants" have an "alias" whereas the lower ones have the box number as correct address for the state i .

The implementation has the following steps:

1. Choose the box i using $i = \text{int}(q \cdot \text{ran}) + 1$ with a random number $\text{ran} \in [0, 1[$.
2. If $\text{ran} < P_{limit}^i$, choose the new state as i , otherwise take the new state as $\text{Alias}[i]$.

The consumption time is therefore independent on the number of states. The only limitation is the memory needed to store the arrays. The method to generate the arrays can be found in the ref. [11] and the implementation at our homepage [2]. The gain, using this method in comparison to the standard heat bath, is from one to ten depending on the number of states. In the figures when using this implementation of the heat bath algorithm, we denote it shortly as *AW* for Alias Walker.

5. Restricted Direct Heat Bath

We want now to improve the heat bath algorithm by avoiding to choose the new state identical to the old one. The old state is A , the chosen new state B and the other accessible states C . To find the form of the function f in eq. (4) we start with the heat bath method and get $f(A, B) = \frac{P(B)}{P(B)+P(C)}$. The denominator would be 1 and $f(A, B) = P(B)$ if $P(A)$ were included in the sum $P(B)+P(C)$. For the reverse process starting from B and choosing the state A in the accessible states $A + C$, we have $f(B, A) = \frac{P(A)}{P(A)+P(C)}$.

The implementation of the algorithm is therefore:

1. Choose B in $B + C$ using heat bath method, see above.
2. Accept B if $\frac{P(B)+P(C)}{P(A)+P(C)} \geq \text{ran}$ according to eq. (4).

We call this algorithm the restricted heat bath or DHB_δ . For two states as the Ising ± 1 spins, this algorithm is equivalent to the restricted Metropolis one Me_δ .

6. Restricted Direct Heat Bath with Walker's Alias

Finally, as above we make use of the Walker algorithm to accelerate the simulation. We call this algorithm the restricted Alias Walker Hasting Algorithm or abbreviated AWH_δ . The arrays to store the values calculated before the simulation are q times larger than for the AW algorithm because they depend on the actual state which can take q values.

We treat thereafter the following discrete spins: Ising ± 1 , Blume-Capel model, Potts model and clock model, and compare the efficiency of each algorithm.

B. Ising ± 1 spins

We consider here the standard Ising spin system. The spins $S_i = \pm 1$ are under the influence of a local field h generated by the neighboring spins. They have an energy

$$E_i = -T \cdot h \cdot S_i \tag{5}$$

with the temperature T and the local field

$$h = \frac{J}{T} \sum_{\langle j \rangle} S_j \tag{6}$$

where the sum is over the neighboring spins. The probability $e^{-E_i/T}$ for the orientation of the spin S_i can be written without normalization as

$$P(\pm 1) = e^{\mp h} . \quad (7)$$

Following the last section we discuss the various algorithms and their implementations for the Ising spins accessible at our homepage [2].

Since there are only two possible states the restricted heat bath DHB_δ and the restricted Metropolis Me_δ algorithms are the same. Moreover no Walker aliases are needed. This is different for a multi-spin update for four spins on a square with $2^4 = 16$ possible configurations. Each of the four spins has two neighbor spins outside which contribute to h the values $-2/T$, 0 or $2/T$. We implement for this case both the heat bath AW_4 and the restricted heat bath $AWH_{4\delta}$ algorithms using Walker method.

We put the results of the simulations for a square lattice with a size $L = 10$ in fig. 1. The integrated autocorrelation times τ (see [7] for its determination) are displayed in fig. 1(a) for comparing the different algorithms. The maximum at the critical temperature T_c is indicated by the black squares. As to be expected $\tau_{Me} > \tau_{DHB}$ because the heat bath method chooses the new state according to its probability. This property is general and therefore also $\tau_{DHB} > \tau_{DHB_\delta}$ because the new state is better chosen by the restricted method DHB_δ than by the direct method DHB .

For Ising spins this is not difficult to analyze. Imagine that the spin state is -1 and the local field h positive. The probability to get to the $+1$ state is $e^{-h}/(e^h + e^{-h}) = 1/(e^{2h} + 1)$ with the heat bath DHB whereas simply e^{-2h} for the restricted heat bath DHB_δ . Since $e^{-2h} > 1/(e^{2h} + 1)$ an Ising spin is more often flipped in the latter case. Similarly if the actual state is $+1$, the probability to get the state -1 is $1/(e^{-2h} + 1) < 1$ with the heat bath DHB and strictly 1 with DHB_δ or the equivalent restricted Metropolis procedure. These differences are small if $h \gg 1$ but become noticeable for smaller h . For the two-dimensional ferromagnet on a square lattice small means already the critical temperature where a third of the flips occurs for $h = 0$. This fact explains also the difference in the acceptance rate between DHB and DHB_δ shown in fig. 1(c),

It is evident by comparing fig. 1(a) with fig. 1(c) that a bigger acceptance rate corresponds to a smaller autocorrelation time. One can also see that a two times smaller acceptance rate double more than twice the autocorrelation time. The reason may be that some parts of

the lattice flip more than average, some parts less, and these slow spins have a dominant influence on τ . We will come back to this point when we study the continuous spins.

The multi-sites heat bath AW_4 and $AWH_{4\delta}$ improve the situation compared to the single site DHB , but are somehow less efficient than the DHB_δ or the restricted Metropolis Me_δ procedure. This procedure, usually called simply “Metropolis” in the literature is therefore the most efficient algorithm for ± 1 Ising spins.

For the judgment of the numerical efficiency the important parameter is not the autocorrelation time, but the actual time the computer consumes. If an algorithm \mathcal{A} has a τ two times smaller than an algorithm \mathcal{B} , but is ten times slower to execute, it is better to use the algorithm \mathcal{B} . We take as consumption time the product of the autocorrelation time τ by the actual simulation time of one Monte Carlo step.

The simulation time is plotted in fig. 1(b). For one MC step Me , DHB and $DHB_\delta = Me_\delta$ algorithms use almost the same time. As to the results for AW_4 and $AWH_{4\delta}$ the four spins algorithm AW_4 is 40% faster than the three previous one spin algorithms since the four spins are flipped simultaneously. The benefit is lost with the $AWH_{4\delta}$ method even if implementations are almost the same. The disadvantage is due to the limited fast cache memory of the processor with an access time 10 times faster as ordinary memory. Using the Walker’s method the informations to be stored becomes 16 times larger for $AWH_{4\delta}$ than for the AW_4 . For the same reasons, when the temperature increases, the number of configurations simulated increases, and the number of variables stored in the cache memory overflows its capacity. This explains the behavior of $AWH_{4\delta}$.

Finally we show in fig. 1(d) the consumption time of the computer to compare the efficiency of each algorithm. At the critical temperature, the restricted heat bath DHB_δ and the restricted Metropolis Me_δ are 4 times more efficient than the Metropolis Me , and 2.5 times more efficient than the heat bath DHB . It is interesting to compare the efficiency of AW_4 and $AWH_{4\delta}$. The last algorithm has a smaller autocorrelation time than the former, but a larger time of simulation and therefore it is less efficient. Even the AW_4 is not really more efficient than $DHB_\delta = Me_\delta$. Therefore for the ± 1 Ising spin the restricted heat bath or Metropolis algorithm should be used since also a single-site algorithm is simpler to program.

We checked that these results do not change markedly as a function of the size. This is expected since all the algorithms we compare are local, the autocorrelation times have the same behavior and their comparative efficiency remains the same.

In addition we tested the two and three-dimensional antiferromagnetic triangular lattices and the three-dimensional $\pm J$ spin glasses on a cubic lattice. The results are alike and even more in favor of the $DHB_\delta = Me_\delta$ compared to DHB and Me . This is so because the number of zero local fields is more important in these cases, up to 30% at low temperatures for the triangular antiferromagnetic lattices.

C. General Ising spin and the Blume–Capel model

The Blume–Capel model is defined by a Hamiltonian

$$H = -J \sum_{\langle ij \rangle} S_i S_j + \Delta \sum_{\langle i \rangle} S_i^2 \quad (8)$$

with the first sum over nearest neighbor pairs and the second one over all N spins. Each spin has $2S+1$ components $S_i = -S, -S+1, \dots, S$. This model can be used to describe a mixture of He_3 and He_4 . Initially the model had three components [12]. Later the model was extended from $S = 1$ to $S = 3/2$ [13] and could be generalized to any S .

We apply the single-site algorithms defined previously. For this model, contrary to the Ising model, the restricted Metropolis Me_δ is no more identical to the restricted heat bath DHB_δ and its corresponding Walker method AWH_δ .

In fig. 2 we present results for this model. The graphs for acceptance rate are shown in fig. 2(a), equivalent to the Ising case in fig.1(c). The simulations are for a square lattice of size $L = 10$ for $S = -1, 0, 1$ with $\Delta = 0$. AWH_δ and DHB_δ have the same acceptance rate since they are only variants of the same restricted heat bath algorithm. This is also the case for the heat bath algorithms DHB and AW . The autocorrelation times τ , not shown here, follow a similar pattern as the acceptance rates and therefore $\tau_{AWH_\delta} = \tau_{DHB_\delta} < \tau_{AW} = \tau_{DHB} < \tau_{Me_\delta} < \tau_{Me}$.

In fig. 2(b) the consumption time is shown for the same model, that is $S = \pm 1, 0$ and $\Delta = 0$. At the critical temperature the restricted heat bath algorithms DHB_δ and AWH_δ have the same efficiency, whereas the heat bath algorithms DHB and AW are 25% less efficient and the restricted Metropolis method 50%. The Metropolis algorithm, usually used in the literature is 2.7 times slower. The consumption time at the critical temperature if $\Delta \neq 0$ in the fig. 2(c) exhibits similar features as seen in fig. 2(b), which are even more pronounced in favor of the restricted heat bath.

In fig. 2(d) the consumption time at the critical temperature for $\Delta = 0$ is displayed as function of S . For very large S the restricted and not restricted algorithms give similar autocorrelation times. However, the simulation times for one step are not the same for the algorithms and in particular the Walker algorithm AW and AWH_δ should give better results. For intermediate values of S shown we observe that all the heat bath algorithms for $S \geq 3/2$ are almost equivalent and much more efficient than the restricted Metropolis Me_δ , which is more than 1.5 times slower, and the simple Metropolis Me more than a factor 2.3.

Since the algorithms are local these results hold for other lattices as well and larger sizes. In the next section some results are shown as a function of the size and for different lattices.

D. Potts model

The Potts model [14] is defined by a Hamiltonian:

$$H = -J \sum_{\langle ij \rangle} \delta_{q_i q_j} \quad (9)$$

$\delta_{q_i q_j}$ refers to the q state Potts spin with $\delta_{q_i q_j} = 0$ when $q_i \neq q_j$ and $\delta_{q_i q_j} = 1$ when $q_i = q_j$. For the two-dimensional square lattice with ferromagnetic interactions the transition is of second order for $q \leq 4$ and of first order if $q > 4$. This model is still extensively studied in particular with antiferromagnetic interactions [15].

In fig. 3 we plotted the result for the ferromagnetic three state Potts model ($q = 3$) on a square lattice (2s). The system size is $L = 20$. The results are very similar to the Ising two states case, but as clearly seen in fig. 3(b) the Walker method improves the situation compared to the heat bath by a gain of 30% for the direct heat bath and of 50% for the restricted heat bath. From the fig. 3(d), at the critical temperature the restricted heat bath with Walker's alias AWH_δ is 50% more efficient than the same heat bath without Walker's alias DHB_δ , and more than two times better than the heat bath procedures AW and DHB . The factor increases to more than three for the restricted Metropolis Me_δ and to six when Metropolis Me is used. Obviously this ratio depends on the implementations and the ones used here are accessible at [2].

For the same model and at the critical temperature in fig. 4(a) the graphs for the consumption time are shown as a function of the system size L . One observes that the results do not depend on the size in a marked way.

In fig. 4(b) we show the consumption time at the critical temperature as a function of q . For $q = 10$ the system exhibits a strong first order transition and we have used the multicanonical algorithm [6] in combination to the local algorithms. For large q restricted algorithms are equivalent to non restricted ones. The heat bath algorithms are much better, ≈ 8 times faster for $q = 10$, than the Metropolis ones. We observe an increase of the consumption time for AWH_δ algorithm for $q = 10$. This is due to the size of arrays needed to store which exceeds the possibilities of the cache memory. For more details see the Ising ± 1 section and the problems for the $AWH_{4\delta}$.

Since all the algorithms are locals the results hold for other lattices and interactions as well. In the fig. 4(c) and fig. 4(d) we plotted the results for the acceptance rate and the consumption times for the anti-ferromagnetic three state Potts model on a three-dimensional cubic lattice (3ca). We get similar results at the critical temperature with a gain of four when we compare the AWH_δ to the Metropolis algorithm Me .

E. Clock model

The q state clock model [16, 17] is a discrete version of the continuous XY model. The Hamiltonian may be written as

$$H = -J \sum_{\langle ij \rangle} \cos[2\pi(q_i - q_j)/q] . \quad (10)$$

For $q = 2$ this is the Ising model and for $q \rightarrow \infty$ the XY model. An example for $q = 3$ is shown in fig. 5(a).

We adapt as before different local algorithms to this model. In fig. 5(b) we plot an example for the Walker “boxes” described in the section ref III A 4. For this model it is advisable to change the restricted Metropolis method in the sense that a new state q^{new} is confined to the neighborhood of the old state q^{actual} . The simplest way is to take the new position within the limits $q^{actual} - \delta \leq q^{new} \leq q^{actual} + \delta$ with δ varying from 1 to $q/2$.

In fig. 5(c) the autocorrelation time is displayed for the 10 state clock model with ferromagnetic interactions on a square lattice (2s) as a function of the temperature $T \propto 1/h$ and δ . At low temperatures the best algorithm is the one which tests only new states close to the actual one and at high temperatures it is better to test all possible states. At temperatures between an intermediate δ works best.

Before looking at fig. 5(d) we turn to fig. 6. The model tested there is the six state clock model on the two-dimensional square lattice (2s) of size $L = 10$ with ferromagnetic interactions. It is clear that the Walker method improves considerably the heat bath methods as can be seen in fig. 6(b). Obviously this depends on the implementations and the ones used in these figures are accessible at our homepage [2]. The gains at the critical temperatures (there are two critical temperatures [16]) are quite appreciable in using the heat bath Walker method *AW*. This method is at least four times faster than the Metropolis methods as can be seen in fig. 6(d). In the figures the $sl Me_{\delta^*}$ corresponds to the optimal choice of δ for each temperature.

Now we come back to the fig. 5(d). The consumption times at the critical temperature (the higher temperature of the two critical temperatures) are displayed as function of the number of states. Whatever q is, we observe that the Walker heat bath methods are much more efficient than any other method. Moreover for large q we notice that the restricted Walker heat bath *AWH $_{\delta}$* algorithm becomes less efficient than for low q . The reason is that the arrays become too big to be stored in total in the cache memory, a problem we encountered before (see the Ising \pm section). Interesting is also the result for the $q = 2$ case corresponding to the Ising model. We should get identical results for *AWH $_{\delta}$* and *Me $_{\delta}$* since they are the same algorithm in this case. Indeed the same autocorrelation times are found but the simulation times differ and therefore also the consumption times. The reason is that our implementation which treats any q does not use special features of the $q = 2$ case. Again the reader should be aware that a good implementation is as important as a good algorithm.

IV. CONTINUOUS SPINS

We study now continuous spin systems. The Hamiltonian h should have the form

$$H = -T \sum_i \mathbf{h}_i \cdot \mathbf{S}_i \quad (11)$$

similar to (5) and (6) with

$$\mathbf{h}_i = \frac{1}{T} \sum_j J_{ij} \cdot \mathbf{S}_j . \quad (12)$$

A magnetic field term or any other potential function depending only on norm of the spin S_i can be added. We note that it is possible to write the dipolar spin spin interaction this

way. This form is dictated by most of the improved simulation methods we are going to discuss. For more details about this limitation we refer to the section IV I.

The probability to find the spin i in the state \mathbf{S}_i is given by the Boltzmann factor

$$\begin{aligned} P(\mathbf{S}_i) \cdot d\mathbf{S}_i &= e^{\mathbf{h}_i \cdot \mathbf{S}_i - h_i} \cdot d\mathbf{S}_i \\ &= e^{h \cdot x - h} \cdot dx \quad \text{for continuous Ising spins } x \in [-1, 1], \end{aligned} \quad (13)$$

$$= e^{h \cdot \cos x - h} \cdot d\Omega \quad \text{for } O(N) \text{ spins with } N \geq 2 \quad (14)$$

with

$$d\Omega = dx \quad \text{for } N = 2 \text{ with } x \in [-\pi, +\pi], \quad (15)$$

$$= \sin x dx \cdot dy \quad \text{for } N = 3 \text{ with } x \in [0, \pi] \text{ \& } y \in [0, 2\pi], \quad (16)$$

$$= \sin^2 x dx \cdot \sin y dy \cdot dz \quad \text{for } N = 4 \text{ with } x, y \in [0, \pi] \text{ \& } z \in [0, 2\pi] \quad (17)$$

and similarly for $N > 4$. In eq. (13) and (14) the suffix i has been dropped. The additional factor e^{-h} in the definition of the probability P is a kind of normalization.

A. Simulation methods

In this section we will present the methods to be tested on continuous spin systems. The starting point are again eqs. (2-4).

1. Metropolis algorithm

As for discrete spins, the easiest algorithm to implement is the Metropolis method *Me*. It consists of choosing randomly new spin directions and applying the condition (4). For $N \leq 3$ this is not a difficult task. However for $N > 3$ we cannot integrate and invert the weight of $d\Omega$ in Eq. 17. In this case the standard procedure is to calculate the new spin direction using Gaussian random numbers. More details about the different spin types will be found in the corresponding section. For any system the Metropolis procedure is much less efficient, at least by a factor two, than the algorithms we will discuss below.

2. Restricted Metropolis algorithm

The restricted Metropolis algorithm Me_δ is here defined in a similar way as for the clock model in section III E. The new state is chosen around the actual one restricted by $x^{actual} - \delta \leq x^{new} \leq x^{actual} + \delta$ using Hasting's method (4). This method is usually applied for the XY spin $N = 2$, but could be used for any $N > 2$. The results obtained are better than for the Metropolis algorithm but still this method is less efficient than the ones introduced further down.

3. Direct Heat Bath

The direct heat bath *DHB* can be used only for continuous Ising spins $-1 \leq S < 1$ and Heisenberg spins with 3 components putting simply $f(B) = P(B)$ in (3). The probability is for both cases eq. 13, that is $P(x) \cdot dx = e^{h \cdot x - h} \cdot dx$ with $x \in [-1, 1[$. The cumulative probability F given by the normalized integral of P is then

$$\begin{aligned} F(x) &= \frac{\int_{-1}^x P(\tilde{x}) d\tilde{x}}{\int_{-1}^{+1} P(\tilde{x}) d\tilde{x}} \\ &= \frac{e^{h \cdot x} - e^{-h}}{e^{+h} - e^{-h}} \end{aligned} \quad (18)$$

so that $0 \leq F(x) < 1$. In fig. 7(b) $F(x)$ is plotted. From a random number $F = \text{ran}$ between 0 and 1 one can then determine $-1 \leq x < 1$ by inverting (18):

$$x = 1 + \frac{1}{h} \cdot \log((1 - e^{-2h}) \cdot \text{ran} + e^{-2h}) . \quad (19)$$

This formula has been used for an implementation [18] which actually is easier than for the discrete spins described in the previous section III A 3. With a slight modification one can improve the efficiency especially for large h or low temperature. One generates a value for x in the limit $-\infty < x < 1$ by

$$x = 1 + \frac{1}{h} \cdot \log(\text{ran}) \quad (20)$$

and exclude the values outside the range $[-1, 1]$. This procedure must be iterated until one obtains a value between $-1 \leq x < 1$. This way one does not need to calculate e^{-2h} but a number of choices are rejected and additional random numbers must be generated. One assumes here that h is positive so that the probability $P(x) \propto e^{x \cdot h}$ can be extended

to arbitrary negative values of x . If h is negative one has to change the sign and put $x \Rightarrow x \cdot \text{sign}(h)$. At the critical temperature and below typically one has $h > 1.5$ for various models and the efficiency increases by 25% using the simpler rule (20) instead of (19).

For vector spin models with $n = 2, 4$, and more components the direct heat bath method cannot be applied since the weights are too complicated for a simple integration. One is therefore forced to choose another form for the function f in Eq. 3 and use the rejection method. The choice is very broad and many functions have been tried especially for XY -spins with two components. However, the function chosen are particular for each model. We introduce below three completely general algorithms applicable to any model with an energy of the form given in (11-12).

4. Fast linear algorithm

For an efficient heat bath simulation a function $f > P$ should be chosen for which the integral is easy to determine and also the inversion poses no problem. For a maximum gain in simulation time we find that the best choice is a function with n steps. For an example see fig. 7(a) and (c) where we present choices of step functions for the continuous Ising spin S ($-1 \leq S < 1$) and $h = 5$. The idea is to use this together with the Walker algorithm or a variant of it. We first describe the method, called the Fast Linear Algorithm (*FLA*), in detail.

a. h is constant We first consider the case $h = \text{const}$ where h is defined in eq. 12, and then show later how to deal with the real situation where h can vary.

The function f is made of n constant parts f_i . We choose the f_i with two conditions:

$$f_i = \text{maximum of } q(x) \text{ in the interval } [x_i, x_{i+1}], \quad (21)$$

$$f_i \cdot (x_{i+1} - x_i) = a, \quad (22)$$

with the constant area a to be determined. For an example see the fig. 7(a). The first equation ensures that f is always greater than q . The second is useful for a simple and faster way to invert the cumulative probability F . Indeed we see that F is composed of n intervals of straight lines (integration of n constant functions). With (22), all intervals are equal as shown in fig. 7(b). Therefore, only a few steps are necessary to invert F . This is done as follows.

Choosing a random number between 0 and 1, we find the interval corresponding i

$$i = \text{int}(n \cdot \text{ran}) \quad (23)$$

where int means the conversion from real to integer. Having i , it is not difficult to find x that we are looking for:

$$x = x_i + (n \cdot \text{ran} - i) \cdot (x_{i+1} - x_i) . \quad (24)$$

Since we use only conversions and simple operations, this method is extremely fast. We come back to this point later when we conjecture that it is impossible to find a faster algorithm for this class of problems. Moreover, for $n \rightarrow \infty$ the acceptance rate, i.e., the area of P divided by the area of f between $[-1 : 1[$, tends to 100%. Typically with n being equal to some hundreds one obtains a rejection rate ($= 1 - \text{acceptance rate}$) of few percents.

Technically, we find the $\{x_i\}$ and the $\{f_i\}$ using (21-22) and store the value of a and $\{x_i\}$. This must be done once before the Monte Carlo simulation begins. Then apply (23) and (24) at each Monte Carlo step, calculating f_i using (22).

To determine the $\{x_i\}$ we use an iterative procedure. First we fix a . Next, using (21) and (22), we calculate the corresponding $\{x_i\}$ and $\{f_i\}$. When $x[n] > 1$ we reduce a , otherwise we increase it. The procedure is stopped when $1 \leq x[n] \leq 1 + \epsilon$, with ϵ being the accepted error. Then, we fix $x[n] = 1$ and $f_{n-1} = \frac{a}{1-x[n-1]}$. Since ϵ is positive, f_{n-1} obeys (21). One possibility is to put the initial value of a at $a = A/n$, A being the area of $P(x)$ between $[-1, 1]$ calculated numerically.

b. h is variable Now we have to consider the case where h is no longer constant. We notice $P_{h_1} > P_{h_2}$ if $h_1 < h_2$ with h_i the norm of the vector \mathbf{h}_i , therefore $h_i \geq 0$. We divide the possible range of variation of h in M parts corresponding to h_1, h_2, \dots, h_M and use the table calculated at h_j for $h_j \leq h < h_{j+1}$. Due to this procedure the acceptance rate decreases. We decide to choose the $\{h_j\}$ so that the rejection rate is less than a threshold using:

$$\frac{\text{area of } P_{h_j} - \text{area of } P_{h_{j+1}}}{\text{area of } P_{h_j}} = \text{threshold} . \quad (25)$$

The area of P_h is calculated numerically.

However, the values $\{h_j\}$ are not linearly distributed. Therefore, we create a new table table_h with K elements. In each Monte Carlo run we calculate the value k with a conversion

from real h to integer k and the `tableh` gives us the value of h_i . More specifically:

$$k = \text{int}(K \cdot (h - h_0)), \quad (26)$$

$$h_i = \text{table}_h[k], \quad (27)$$

where h_0 is the first value of h_j . The `tableh` has to be filled before the beginning of the Monte Carlo simulations. K , the number of elements of the table, is free, but must be large enough to be able to differentiate the h_j .

In summary, we have a way to generate the value x with a probability $f(x)$ using (26), then (27), then (23) and finally (24). Using this value of x we apply the rejection method, i.e. accept the new value if $\frac{P(x)}{f(x)} \geq \text{ran}_2$, where ran_2 is a random number in the interval $[0, 1[$. We call this algorithm the Fast Linear Algorithm because we use only linear equations. Few steps are necessary to obtain the final value x looking at the C program given at our homepage [2].

c. Advantages and flaws First we would like to argue that no other algorithm using the rejection method could be faster than the Fast Linear Algorithm.

The rejection method needs two uniformly distributed random numbers at each Monte Carlo step. Step 1 is to get a value x from a known cumulative of the test function f and step 2 is to compare the value $f(x)$ to the probability. To compare different algorithms using this method, it is enough to calculate the time necessary to perform step 1 and step 2 without considering the time to produce the random numbers since it will be the same for all algorithms.

The consumption time can be estimated in comparing the various possible operations executed by the computer. We take the following equivalences: basic operation (`*`, `+`, ...) = 1 unit, conversion from real to integer (`int`) = 3 units, (`if`) = 3 units, square root (`sqrt`) = 6 units, and calculating a function like cosine, exponential or logarithm = 13–18 units. These estimates are only approximate, but sufficient for comparing the different algorithms.

To apply the *FLA* one needs two conversions from real to integer according to eq. (23) and (26), and a few basic operations like additions, multiplications, and the use of tables. If we count the time necessary for our algorithm very roughly, we get 20 “units”. Therefore, the time necessary for one step of the *FLA*–algorithm is comparable to the time needed to calculate one function. Another algorithm, to be as fast as *FLA*, should use only once a calculation of a function. However, in most of the cases, it will never reach such a high rate

of acceptance comparable to *FLA* of nearly 100%. Therefore the algorithm *FLA* should be always the fastest algorithm. This conclusion holds only when the rejection method is used, not for the heat bath methods when the probability can be integrated and inverted as for a classical Heisenberg model. However, even in this case it will be shown in the following that this heat bath algorithm will not be faster than the *FLA* algorithm.

We note another advantage of this method. It is completely general and can be applied to all types of probabilities. Moreover, we have introduced the *FLA* with a probability on a fixed range $[-1, 1[$. However, it is possible to handle also the case of an infinite range with a somehow more complex program, as can be seen in the section dealing with the Ising ϕ^4 model.

The only flaw of *FLA* is that a certain amount of memory must be available to store the tables. For a Hamiltonian which can be factorized like in eq. (11–12) there are two variables, x and h , to handle. Typically we get files which are less than 100 Kb for a rejection rate of about 15% percents. If one wants to decrease this rate the size of the tables increases and the cache memory could become too small to store the arrays. A test of the maximum number of steps which minimize the consumption time is needed at each simulation. See for an example fig. 8(b).

5. Walker's Algorithm

The last algorithm is very efficient, but it is not so easy to calculate the $\{x_i\}$ and it becomes really complex in presence of more variables x_i, y_i, \dots . In this case the Walker algorithm could provide a good solution. The only difference between the Fast Linear Algorithm (*FLA*) and the Walker algorithm (*AW*) is the choice of x_i . Instead of (22) we choose the x_i at fixed interval, for example on the fig. 7(c) the dashed line (“*AW* without x_H ”). Another possible choice to avoid to get a lot of informations in the region where the probability is almost zero is to choose $x_1 = x_H$ and the others x at fixed intervals between x_1 and 1 (“*AW* with x_H ”).

Whatever the choice is, since (22) is no more valid, we cannot use only (23) to calculate i . We must use the Walker's alias introduced previously (section III A 4). We must calculate the integral of each step function, i.e. the area $f_i \cdot (x_{i+1} - x_i)$. Walker's algorithm is used to divide them in n equal boxes as shown in fig. 7(d) for the step function “*AW* with x_H ”

shown in fig. 7(b). During the simulation, we have to use, as for the discrete spins, an `if` condition to choose the correct “state”. Therefore in addition of (23) we must use:

$$\text{if}(\text{ran} > P_{limit}^i) \quad i = \text{Alias}[i]. \quad (28)$$

And (24) must be replaced by

$$x = x_i^{box,ini} + \text{ran} \cdot (x_i^{box,fin} - x_i^{box,ini}) \quad (29)$$

with $x_i^{box,ini}$ and $x_i^{box,fin}$ are the limit for each box and “state”. Otherwise the algorithm is similar to the *FLA*.

The difference of this algorithm and the *FLA* is that we have to store much more data in the arrays. Precisely we have to save the $\{P_{limit}^i\}$, $\{x_i^{box,ini}\}$, $\{x_i^{box,fin}\}$, $\{\text{Alias}[i]\}$ and also $\{f_i\}$ to apply the rejection method. This must be compared to a and $\{x_i\}$ for the *FLA*. As a consequence the arrays are 6 times bigger for the *AW* than for the *FLA*. To be efficient arrays must be stored in the cache memory and therefore the *AW* is less efficient than the *FLA*. For example see fig. 8(d) and fig. 11(b).

However the arrays are very easy to create contrary to the ones for the *FLA*, even with more than one variable. We will present two examples with two variables below when treating Heisenberg spins with a ϕ^4 potential.

6. Walker’s Algorithm with Hasting’s method

Another advantage of the Walker algorithm over the *FLA* is that we can use Hasting’s method. Indeed to apply this last method we need to be able to get not only $F^{-1}(\text{ran})$ but also $f(x^{actual})$ as seen in the Eq. 4. To obtain easily $f(x^{actual})$ we need a simple law for x_i , the simplest being the $\{x_i\}$ distributed at constant intervals. Then we use the Hasting’s method (4) in combination with the Alias Walker. We call it, as before, the Alias Walker Hasting (*AWH*) algorithm.

One big advantage of the Hasting’s method compared to the heat bath-rejection method is that we do not need to choose the function f bigger than the probability P . This proves very useful if the Hamiltonian cannot be factorized like $H = \mathbf{h}_i \cdot \mathbf{S}_i$ (11). In this case the *FLA* cannot be applied but the present method works.

In the next section we present the vector spin with dimensions N from 1 to 6 separately. We try to be as complete as possible in order that the reader can use the proposed methods easily. For each case the C programs are accessible at our homepage [2].

B. Continuous Ising spins $-1 \leq S < +1$, $N = 1$

The continuous Ising spin varies from -1 to +1 with an uniform probability so that the Boltzmann weight according to (13) is

$$P(S_i) \cdot dS_i = e^{h \cdot x - h} \cdot dx, \quad x \in (-1, 1). \quad (30)$$

We explain in more detail the results for this first example of continuous spins since the vector spin cases $N > 1$ discussed later will be technically similar. We restrict ourselves to three types of algorithms.

The first is the Metropolis algorithm Me where one chooses the new value x^{new} uniformly between -1 and 1. This value is accepted with a probability $P(x^{new})/P(x^{actual})$ according to eq.(4) otherwise the old value x^{actual} is kept. To gain a better understanding how this procedure works we turn to fig.7(a) where the probabilities for a local field $h = 5$ and $h = 10$ are plotted. The Metropolis choice for the function $f_{Me} = "1"$ is also shown. Since Hasting's method is used, the function f is automatically renormalized to $P(x^{actual})$. If $P(x^{new}) \geq P(x^{actual})$ the new state is always accepted, which corresponds to $x^{new} \geq x^{actual}$. Otherwise for $x^{new} < x^{actual}$ the new state is taken with a probability $P(x^{new})/P(x^{actual})$. Graphically the acceptance rate is equal to the ratio of the areas under $P(x^{new})$ and under the straight line $f_{Me} = P(x^{actual})$ for $f > P$. If the local field h increases or the temperature decreases, this ratio decreases tending to zero for low temperatures as can be seen in the fig. 7.

The second method, the heat bath DHB , does not have this defect. Formula (19) is used to find the new value x^{new} . Here the rate of acceptance is 1. Updating with formula (20) instead creates difficulties since small local fields occur too frequently. The cumulative probability F is displayed in fig.7(b).

The third type of simulation is Walker's method including the Fast Linear Algorithm FLA , the Alias Walker algorithm AW and the Alias Walker Hasting algorithm AWH . For the two last algorithms we choose x_1 with $P(x_1) = 0.01$ and the others $\{x_i\}$ are fixed at constant

intervals between x_1 and 1. We plot such a construction in fig. 7(c) under the label “AW with x_H ”. This somewhat arbitrary choice of x_1 is recommended since for $-1 < x < x_1$ the probability is small enough and therefore it is not necessary to provide detailed informations on this range. The corresponding Walker aliases are plotted in fig. 7(d).

The *FLA* fixes automatically this last problem. In fig. 7(a) the step function f_{FLA} is shown for five bins and the corresponding cumulative probability in fig. 7(b). There the dashed lines are equidistant because of the condition (22). In this method the acceptance rate is the ratio of the area under P and under f_{FLA} in fig. 7(a). This ratio can be made close to 1 by increasing the number of bins. The deviation from this ideal value we will denote by “error” in the following.

We compare now in fig. 8 the efficiency of the different algorithms for an antiferromagnet on a three-dimensional stacked triangular lattice (3t). A system size of $L = 6$ is sufficient for the test. Fig. 8(a) shows the refusal rate of *FLA*, *AW* and *AWH* as a function of the “error” given as input to the programs `create_01.out` and `create_01_walker.out` [2] used to create the arrays. The actual refusal rate is approximately only half of the “error” value for the *FLA* and the *AW*, and one fourth for the *AWH*. It is worth to note that *AW* and *AWH* use the same information stored in an array. The difference is that the Hasting algorithm is automatically renormalized to the value $P(x^{actual})$ as explained before, and therefore it fits the probability distribution P better.

The fig. 8(b) shows the consumption time for the last three algorithms at $T = T_c \approx 1.2$. The three curves have a similar behavior. At first, if the error decreases by increasing the number of bins the refusal rate will decrease, and therefore the consumption time decreases also. However if the number of bins becomes too large, the array cannot be kept in the fast cache memory, the time of simulation increases and the gain in the acceptance rate does not compensate the loss in the simulation time of one MC step. We remind the reader that the consumption time is defined as the product of the simulation time of one MC step and the autocorrelation time. This last quantity being shorter for a higher acceptance rate. We observe that the *FLA* has the smallest consumption time because the array to be stored is six times smaller.

We display in fig. 8(c) also the dependence of the acceptance rate for the various algorithm on the temperature or more precisely on the inverse of the local field $1/h \propto T$. The number of bins for the algorithms (*FLA*, *AW* and *AWH*) is chosen to minimize the consumption

time. The acceptance rate of Me goes to zero when the temperature decreases as has been discussed before. As a consequence the autocorrelation time (not shown) increases without limit. As can be seen in fig. 8(c) the AWH acceptance rate is larger than the AW rate, even if the same array is used. The FLA and the AWH have a high acceptance rate for any h comparable to the acceptance rate of the direct heat bath DHB which is strictly 1.

There is a difference between the acceptance rate of the Hasting algorithms AWH and Me on one hand, and the heat bath algorithms AW and FLA on the other hand. In the first case, after a refusal the same spin is kept. In the last case a new spin is chosen until it is accepted, and therefore the new state is always different from the old one. We will see the implication of this fact in the next paragraph.

The most important parameter in numerical simulations, the consumption time, is displayed in fig. 8(d). Clearly the FLA algorithm is the most efficient one even compared to DHB . It is interesting to compare the result for Me with the inverse of the acceptance rate multiplied by the ratio of the times of simulation for Me and FLA , plotted with the symbol $\%$. If the system were composed of only one spin, the two lines would collapse. We observe that the consumption time for Me is above the $\%$ line. Indeed, if the spins of some parts of the lattice are flipping more than the average, some group of spins flip much less than the average and these last spins have a strong influence and the autocorrelation time τ , and therefore on the consumption time for the simulation.

We have tested different lattice sizes L in order to check that results discussed do indeed not depend on L , since the algorithms are local ones. For different lattices the only change is the value of the local field h . Looking at our homepage [2] one can see the nearly collapsing curves for an anti-ferromagnet on a two-dimensional triangular lattice (2t) and a ferromagnet on a square lattice (2s).

In the literature, studies on the continuous Ising model are not very common. To our knowledge the most recent study is for two-dimensional ferromagnetic interactions of long range using the Metropolis algorithm [19]. The use of the heat bath methods FLA or DHB would increase the efficiency because an acceptance rate close to 100% is even more important if the interaction is of long range. Since the simulations for the continuous Ising model ($N = 1$) is similar to the Heisenberg case ($N = 3$) all conclusions for the former model hold also for the latter.

C. Ising ϕ^4 model, $N = 1$

In this section we study the Ising ϕ^4 model [20] or Ginzburg–Landau model on a lattice where the spin variable x varies from $-\infty$ to ∞ . The Boltzmann weight is

$$P(S_i) \cdot dS_i = e^{h \cdot x - x^2 - \lambda(x^2 - 1)^2} \cdot dx \quad (31)$$

and in fig. 9(a) this probability is plotted for $h = 1$ and $\lambda = 1.3182$. It is interesting to study this model for its own sake. Here it serves as an example how to cope with the infinite boundaries of the probability distribution in the *FLA*, *AW* and *AWH* algorithms. Cluster algorithms exist for this model but one needs a local algorithm to vary the norm of the spin [20]. The probability (31) cannot be integrated in a simple way and therefore no direct heat bath method is available.

With the restricted Metropolis Me_δ algorithm the new spin x^{new} variable is chosen around the actual one: $x^{actual} - \delta \leq x^{new} \leq x^{actual} + \delta$. Then the Hasting formula (4) is applied with the function $f_{Me_\delta} = 1$ plotted in fig. 9(a). We compare here the efficiency of the restricted Metropolis algorithm Me_δ only with the Fast Linear Algorithm *FLA* which is faster than *AW* and *AWH*.

The *FLA* is slightly different from the one described in the previous section since a first step starting at $x_0 = -\infty$ and a last one ending at $x_n = +\infty$ would lead to a divergence for the cumulative function F . The solution is to take two exponential functions for the first interval $[x_0, x_1]$ and the last one $[x_{n-1}, x_n]$, and otherwise to take a step function for f . An example is given in fig. 9(a) for $n = 11$ steps. Unfortunately the implementation is also a little bit more complicated than previously.

Fig. 9(b) gives the consumption time at different temperature for the *FLA* as function of the “error” given to the program `create_01_Phi4.out` (accessible from our homepage [2]). The best choice is 20% corresponding to $n = 38$ bins.

The fig. 9(c) and (d) display the acceptance rate and the consumption time for a ferromagnet on a cubic lattice (3c) for a system size $L = 6$. We observe that the *FLA* is much more efficient than the Metropolis algorithm. At the critical temperature represented by the squares, the Metropolis Me_δ is almost three times slower than the *FLA*.

Since our algorithms are local, results do not depend on the system size nor on the type of the lattice. For this model there exist cluster algorithms and also an over-relaxation

algorithm [5]. We must employ them in combination (the section devoted to XY spins shows results for the FLA in combination with over-relaxation). Moreover if we are interested in frustrated system there are no more cluster algorithms available and an efficient local algorithm is fundamental.

D. XY and $U(1)$ variables, $N = 2$

The XY spin is a two-dimensional vector of norm one. Since there is an equivalence between the direction of the spin and a phase, both characterized by one angle, XY spin systems and $U(1)$ gauge theory (see for example [21]) have a common basis. Due to the varied interests many algorithms have been tried. We want to compare them to the Fast Linear Algorithm FLA which proves to be the fastest algorithm, and the Walker Hasting algorithm AWH .

The Boltzmann probability is simply

$$P(\mathbf{S}_i) \cdot d\mathbf{S}_i = e^{h \cdot \cos x - h} \cdot dx \quad (32)$$

with the angle x varying between $-\pi$ and π .

Contrary to the probability of the former case $N = 1$ given by (30) the cumulative probability and its inversion is too costly in computer time and consequently no direct heat bath method DHB is possible. One must use the heat bath rejection or Hasting's methods instead.

We have tested first the standard Metropolis algorithms Me for which $f(x) = 1$ in eq.(4). The new angle x^{new} is chosen randomly between $-\pi$ and π and accepted according to the probability P which is shown in fig.10(a) for $h = 4$. If the local field h increase, the probability is more peaked near the origin and the acceptance rate decreases as explained before. The restricted Metropolis Me_δ gives better results. In this case $x^{actual} - \delta \leq x^{new} \leq x^{actual} + \delta$ as indicated in fig. 10(a). For a small enough δ the acceptance rate can increase up to one, but then the spin configuration will change very slowly and the autocorrelation time becomes large. This situation is the same as for the clock model described in section III E.

For the heat bath method many different functions $f(x) > P(x)$ in the interval $(-\pi, \pi)$ have been proposed. For the auxiliary function f of eq.(3) Moriarty [22] proposed an exponential form (Mo), Edwards et al. [23] a Gaussian form (G), and Hattori and Nakajima

[24] an ingenious hyperbolic cosine function (H). For clarity we plotted in the fig. 10(c) these functions together with the probability P for $h = 4$.

In principle the *FLA* and the *AWH* algorithms follow a similar strategy. The *FLA* step function f is shown in fig. 10(a) for 9 bins. As explained before one should choose the optimal number n for the intervals to minimize the consumption time. This is shown for the *FLA* for three different temperatures for an anti-ferromagnet on the three-dimensional triangular lattice in fig. 10(b). With the choice of $n = 56$ bins the Boltzmann weight is sufficiently well approximated by an error of 15% and this choice will be almost independent on the lattice type.

Before looking at fig. 10(d) where the Metropolis procedure is compared to the more efficient *FLA* procedure, it is interesting to compare all the different algorithms just reviewed. Simulations are made for the two-dimensional triangular lattice (2t) and for the spin glass with $\pm J$ interactions on a four-dimensional cubic lattice (4sg). The results are presented in fig. 11 for a system size of $L = 12$ for the 2t-lattice and for $L = 4$ for the 4sg-lattice.

In fig. 11(a) where the acceptance rate is displayed, one observes that the *FLA* has the best acceptance rate followed by the Hattori algorithm. However, the consumption time displayed in fig. 11(b) is the fundamental parameter for a comparison. Then the situation changes dramatically. The *FLA* is still the most efficient of all algorithms with a gain of 60% compared to the Gaussian algorithm G and 200% compared to the Metropolis one Me at the critical temperature. The Hattori's algorithm becomes the worst of all algorithms (at least for $T \geq T_c = 0.514$, see [25]) in spite of a very good acceptance rate. This is due to a very long time of simulation of one MC step since the function f and the cumulative probability are too complicated. This criticism is in agreement with [26].

Fig. 11(c) shows the results at the critical temperature for the Metropolis Me and Me_δ and for the *FLA* algorithms. These algorithms are combined with the over-relaxation algorithm [5] where the number of these additional updates is denoted by OR . The combination allows a gain of a factor two for the *FLA* and three for the Me . The gain in using *FLA* instead of Me is 3 without an over-relaxation step but it decreases to almost 2 with one or two such OR -steps which consume very little additional time. The best number of over-relaxation steps depends on the temperature or the value of the field h and on the lattice size.

Fig. 11(d) displays the consumption time for a spin glass on a four-dimensional cubic lattice (4sg) with $\pm J$ interaction [27]. In combination with the local algorithm the exchange

algorithm [4] is used. There is almost no difference between the heat bath algorithms *FLA*, *G*, *Mo* and *H*, compared to the (2t) case shown in fig. 11(b). Also the Metropolis procedure is “less worse” when used in combination with the exchange algorithm. It is “only” 1.5 times less efficient than the *FLA* at the critical temperature shown by the squares. This factor grows until 2 times for Me_δ or 3 times for *Me* at lower temperatures, one is interested in for the spin glasses. The best simulation technique should use the *FLA* procedure in combination with the over-relaxation and the exchange algorithm.

As discussed before the results do not vary strongly as function of the size. Further results for the three-dimensional antiferromagnetic stacked triangular lattice (3t) and for the two-dimensional ferromagnetic square lattice (2s) can be found in our homepage [2]. They are practically the same, if taken as a function of the relevant variable that is the local field h (12).

We want to come back to fig. 10(d) where the Metropolis algorithm *Me* is compared to the *FLA* for various lattices as function of the temperature. One notices that the *FLA* is the most efficient algorithm for all lattices tested. This result is completely general.

E. Heisenberg spins, $N = 3$

For Heisenberg spins as three component vectors with unit norm the distribution function is according to (14) and (16)

$$\begin{aligned} P(\theta, \phi) \cdot \sin \theta d\theta \cdot d\phi &= e^{h \cdot \cos \theta - h} \cdot \sin \theta d\theta \cdot d\phi \\ &= e^{h \cdot x - h} \cdot dx \cdot d\phi \end{aligned} \tag{33}$$

with ϕ varying from $-\pi$ to π , θ from 0 to π , and $x = \cos \theta$ from -1 to 1 . P is of the same form as (30) for the continuous Ising spin $-1 \leq S < 1$ multiplied by an additional $d\phi$. Therefore all algorithms used for this last model can also be applied to the Heisenberg or $O(3)$ model. In addition we test two other algorithms. The first is the restricted Metropolis algorithm Me_δ where $x^{actual} - \delta \leq x^{new} \leq x^{actual} + \delta$ and the second one the direct heat bath DHB_2 where instead of formula (19) for an update (20) is used.

For testing the algorithms an anti-ferromagnet on a the three-dimensional stacked triangular lattice (3t) is selected. In fig. 12(a) the probability $P(h = 5)$ is shown together with the “steps” the *FLA* procedure is using. The Metropolis function $f_{Me} = 1$ is also dis-

played. In fig. 12(b) the consumption time for the *FLA* for different temperatures is plotted as function of the “error”. From the figure the best choice is where the Boltzmann weight is approximated by an error of 15% which corresponds to $n = 55$ bins.

It is interesting to look also at the acceptance rate shown in fig. 12(c). For the *DHB* the acceptance rate is 1, but not so for the *DHB*₂ variant because of the rejection of value less than -1 using (20).

Fig. 12(d) shows the consumption time for the algorithms. As can be seen the best algorithm is the “new” heat bath *DHB*₂. It is 25% more efficient than the usual heat bath *DHB* and three times better than the Metropolis algorithms at the critical temperature shown by the squares.

F. Heisenberg ϕ^4 model, $N = 3$

In this section we study Heisenberg spins with a norm y varying between 0 and ∞ . A potential depending on y is added so that the Boltzmann probability of (33) is changed to

$$\begin{aligned} P(\theta, \phi, y) \cdot dy \cdot \sin \theta d\theta \cdot d\phi &= e^{h \cdot y \cdot \cos \theta - y^2 - \lambda(y^2 - 1)^2} \cdot dy \cdot \sin \theta d\theta \cdot d\phi \\ &= e^{h \cdot y \cdot x - y^2 - \lambda(y^2 - 1)^2} \cdot dy \cdot dx \cdot d\phi. \end{aligned} \quad (34)$$

We plotted this probability for $h = 2$ and $\lambda = 1.3182$ in fig. 13(a). To study this model for its own sake is an interesting task. Here it serves as an example how to handle at the same time two variables in the probability distribution. We tested four algorithms.

First we apply two single variable algorithms consecutively for the variable x and then for the variable y . We try two restricted Metropolis procedures $Me_{2\delta}$ and also two fast linear algorithms *FLA*₂.

In updating both variables x and y in a single Monte Carlo step we use as a first method a restricted Metropolis algorithm where $x^{actual} - \delta_x \leq x^{new} \leq x^{actual} + \delta_x$ and $y^{actual} - \delta_y \leq y^{new} \leq y^{actual} + \delta_y$. The consumption time is minimized by adjusting δ_x and δ_y to the temperature changes. The second method is the Alias Walker Hasting algorithm *AWH*. We did not use the *FLA* algorithm since it became too difficult to be implemented for two variables. In any case the array would be almost as large as for the *AWH* algorithm since both coordinates x and y for each box must be stored.

In fig. 13(b) we show the consumption time for simulating a ferromagnet on a three-

dimensional cubic lattice for different temperatures using *AWH* algorithm. The number of intervals n_y for the y variable is varied for $n_x = 10$ to find the best value n_y . Similarly a graph could be shown for dependence of the time on the number of bins n_x for the x variable. We found that the best choice is $n_x = 10$ and $n_y = 20$. This corresponds to $n = n_x \cdot n_y = 200$ bins.

In fig. 13(c) and (d) the acceptance rate and the consumption time are shown for all four algorithms. One sees that *AWH* is the best one but almost equivalent in efficiency to the two fast linear algorithms used consecutively *FLA*₂. The Metropolis algorithms Me_δ and $Me_{2\delta}$ are far less efficient.

In conclusion it seems not worth to consider both variables x and y at the same time and it is better to update them consecutively. However, this conclusion may hold only if the probability has a form similar to the one in fig. 13(a). The situation will be different if, for example, there exists two or more peaks in the probability distribution connected by regions of low probability. In this case the *AWH* algorithm should become much more efficient.

G. $O(4)$ spins

The $O(4)$ spin is a four components vector with norm unity. The probability distribution using (14) and (17) is similar to the one appearing in $SU(2)$ gauge theory [28, 29] and has the form

$$\begin{aligned}
 P(\theta_2, \theta_1, \phi) &\cdot \sin^2 \theta_2 d\theta_2 \cdot \sin \theta_1 d\theta_1 \cdot d\phi \\
 &= e^{h \cdot \cos \theta_2 - h} \cdot \sin^2 \theta_2 d\theta_2 \cdot \sin \theta_1 d\theta_1 \cdot d\phi \\
 &= e^{h \cdot x_2 - h} \cdot \sqrt{1 - x_2^2} dx_2 \cdot dx_1 \cdot d\phi ,
 \end{aligned} \tag{35}$$

with ϕ varying from $-\pi$ to π , θ_i from 0 to π , $x_2 = \cos \theta_2$ and $x_1 = \cos \theta_1$ from -1 to 1 . This probability is not integrable in a simple way and therefore no direct heat bath *DHB* can be used.

Three types of Metropolis algorithms are compared. The first is the standard one for $N \geq 4$. The four components are taken randomly using Gaussian random numbers and then are normalized to get a unit vector. We denote this method by Me_G in the figure.

The second one, denoted by Me , we introduce here, will be faster than the Me_G method for not so large N and equivalent in performance to Me_G for $N \rightarrow \infty$. We choose randomly ϕ ,

x_1 and x_2 and accept the last value with a probability $\sqrt{1 - x_2^2} \leq 1$.

The last one is the restricted Metropolis Me_δ . We follow the second Me procedure but restrict the choice of the new value by $x_2^{actual} - \delta \leq x_2^{new} \leq x_2^{actual} + \delta$.

We found three other algorithms in the literature, mainly used in the context of the $SU(2)$ gauge theory. The first one is the Creutz algorithm Cr [28]. It fits P of (35) with an exponential like the Moriarty algorithm in the XY case (see fig.14(a)).

The second one is due to Fabricius et al. [30], which we call Fa . With a change of variables, they fit the probability P depending on x_2 of (35) by the function $\sqrt{1 - x_2} \cdot e^{h \cdot x_2 - h}$, but the price to pay is a more complicated algorithm.

The third Ke is similar to the last one, but is slightly modified to gain in speed. It is due to Kennedy and Pendleton [31].

We have implemented also the FLA procedure. We calculate x_2 and determine ϕ and x_1 randomly. In the final stage we use these values to create a new spin around the local field h . All the implementations of the methods introduced in this section are accessible at our homepage [2].

The results of the simulation are displayed in fig.14 for the three-dimensional anti-ferromagnet on a stacked triangular lattice (3t). Fig.14(a) we show the probability and our function $f_{FLA}(x_2)$ with $n = 20$ bins and $h = 2$. $P(x_2)$ reaches its maximum at $x_2^{max} = (\sqrt{1 + 4h^2} - 1)/2h$ which is useful for the application of formula (21). In the same figure the function of Creutz and the Metropolis probability are also shown.

The fig.14(b) shows that an error of 15% corresponding to $n = 55$ bins is the best choice for the FLA . The acceptance rate is shown in fig.14(c) and in fig.14(d) the consumption time of the various algorithms. Again the FLA algorithm is the most efficient algorithm. At the critical temperature shown by the squares the gain is a factor 5 compared to the Me or Me_δ and reaches even 9 in comparison to the standard Me_G .

For the $SU(2)$ gauge theory we do not have to update ϕ and x_1 , therefore the situation is even more in favor for a simulation with the FLA . In the interesting region $h \approx 1/16$ [31], the gain is of 30% compared to Kennedy's algorithm Ke , 80% to Fabricius's algorithm Fa , and 120% to the algorithm of Creutz Cr .

Since the algorithms are local, the results are valid for different lattices and sizes.

H. $O(N)$ spins

The $O(N)$ spins, that is vectors of unit norm in N dimensions, do not have an experimental realization, but can be helpful for a better understanding of the nature of phase transitions [32, 33]. The probability can be written as

$$\begin{aligned}
 P(\theta_N, \dots, \theta_1, \phi) &\cdot \sin^{N-2}\theta_{N-2} d\theta_{N-2} \cdots \sin \theta_1 d\theta_1 \cdot d\phi \\
 &= e^{h \cdot \cos \theta_{N-2} - h} \cdot \sin^{N-2}\theta_{N-2} d\theta_{N-2} \cdots \sin \theta_1 d\theta_1 \cdot d\phi \\
 &= e^{h \cdot x_{N-2} - h} \cdot (1 - x_{N-2}^2)^{\frac{N-3}{2}} dx_{N-2} \cdots dx_1 \cdot d\phi
 \end{aligned} \tag{36}$$

with ϕ varying from $-\pi$ to π , θ_i from 0 to π , $x_i = \cos(\theta_i)$ from -1 to 1 .

The probability for $O(N)$ spins is not amenable to the direct heat bath *DHB* technique. This problem is similar to the $O(4)$ case with the probability given by (35). In addition for the $O(N)$ case the variables $\{x_{N-3}, \dots, x_2\}$ can also not be dealt with in a simple way. See fig. 15(a-c) where for $N = 6$ the probabilities are shown for x_4 , x_3 and x_2 .

We have used the same Metropolis algorithms as in the previous section, that is the simple Metropolis Me , the restricted Metropolis Me_δ , and the standard one Me_G . For the two first algorithms Me and Me_δ , the $\{x_{N-3}, \dots, x_2\}$ variables are determined using a rejection method: a random number x_n between -1 and 1 is accepted as x_n^{new} with a probability $(1 - x_n^2)^{\frac{n-1}{2}}$. The refusal rate is proportional to the area between the curve “sinus” in fig. 15(b,c) and the curve $(1 - x_n^2)^{\frac{n-1}{2}}$. The x_{N-2} is calculated randomly between -1 and 1 (or between $x^{actual} \pm \delta$) and accepted with Hasting formula (4) with $f = 1$.

In analogy to Moriarty’s algorithm for XY spin, to the heat bath for Heisenberg spin, or to the algorithm of Creutz for $O(4)$ spins, we introduce an exponential algorithm Ex for the x_{N-2} variable. We calculate x_{N-2} using $x_{N-2} = -1 + \frac{1}{h} \log[1 + \text{ran} \cdot (e^{2h} - 1)]$ and accept it with a probability $(1 - x_{N-2}^2)^{\frac{N-3}{2}}$. The others $\{x_n\}$ are calculated in a similar way as for Me .

We want to show that it is profitable to use the *FLA*. For $N = 6$ the best choice corresponds to 15% of error and $n = 55$ bins for x_4 as shown in fig. 15(d). For x_3 and x_2 the *FLA* is also used with 200 bins (see fig. 15(b) and (c) with 10 and 20 bins, respectively). The probability $P(x_{N-2})$ reaches its maximum at $x_{N-2}^{max} = (\sqrt{(N-3)^2 + 4h^2} - (N-3))/2h$ which is helpful for constructing the step function f for the *FLA* with eq.(21).

In fig. 16(a) and (b) we put the essential results for $N = 6$, obtained for an anti-

ferromagnet on a three-dimensional stacked triangular lattice (3t)[32, 33]. In fig. 16(a) the acceptance rate for the different algorithms is shown. We want to point to the differences between Hasting's method (e.g. Metropolis) and the heat bath methods (e.g. *FLA* and *Ex*). In the first case, if the new spin is not accepted, all values x_n and the angle ϕ are discarded. In the other case for the heat bath method one always gets a new state. Therefore the last algorithm becomes much more efficient if the number of values x_n to be calculated increases. In fig. 16(b) one can compare the consumption time for the different algorithms. One sees, that *FLA* is the most efficient of all the algorithms tested.

Fig. 16(c) and (d) contains a summary of results for different spin dimension $1 \leq N \leq 6$, that is the acceptance rate and the consumption time at the critical temperature for an anti-ferromagnet on the 3t-lattice. The algorithms compared are the fast linear algorithm *FLA*, the Metropolis algorithm *Me*, the restricted Metropolis algorithm *Me_s* and the Gaussian Metropolis algorithm *Me_G*. One observes that the *FLA* is more efficient than any Metropolis algorithms and that the advantage is larger for an increasing number of spin components N . This conclusion is totally general and does not depend on the system size nor on the lattice type.

I. Other types of spin Hamiltonians

Until now we only have dealt with Hamiltonians which can be written in the form given by (11) and (12). In fact the Fast Linear Algorithm *FLA* can only be used for this kind of Hamiltonian. However, the Alias Walker Hasting procedure is more flexible.

For example, for a Hamiltonian $H = - \sum_{\langle ij \rangle} (S_i \cdot S_j)^3$ [34] the ground state is a conventional ferromagnetic one and at finite temperatures the spins will still be oriented around the direction of all their neighboring spins. However, one cannot define a local field h as in (12) for this cubic exchange. This means that the *FLA* algorithm or any other heat bath method cannot work. For these methods one needs a function $f \geq P$ and since there is no formula of $P(h)$ definable, one has only the inefficient choice of a constant f equal to the maximum of P . However, Hasting's method is not limited by the condition $f \geq P$. Among these methods the *AWH* algorithm with a choice for f , for example similar to the case with linear interactions we discussed, should offer a possibility for an efficient simulation.

V. CONCLUSION

In this article we have tried to review as completely as possible the available canonical local algorithms for discrete and continuous spin systems. Starting from the difference between Hasting's and heat bath methods we analyzed the algorithm regarding their numerical efficiency. In all cases except the standard Ising case, we could demonstrate that by modifying known algorithms or to construct new ones the efficiency increases compared to the standard ones, in particular compared to the widely known and used Metropolis algorithm.

For discrete spins (Ising model, Blume-Capel model, Potts model and clock model) the best algorithm is a restricted heat bath Walker Hasting algorithm where the new state is chosen by the heat bath procedure among all accessible states excluding the actual one. Then Hasting's method is used to accept or reject the new state. To accelerate the simulation we have proposed Walker's alias method, usually not used in this context.

For continuous spins (continuous Ising spin, XY spins, Heisenberg spin and $O(N \geq 4)$ spins) we introduced different Walker Hasting's methods and the Fast Linear Algorithm. These methods are efficient at all temperatures and achieve a gain at the critical temperature of usually more than two compared to the Metropolis algorithm. For low temperature the gain becomes even larger.

We use arrays heavily to store data calculated prior to the simulation. Therefore the efficiency of the introduced algorithms depend strongly on the amount of fast cache memory of the processor. Since this amount will certainly increase in the future, the algorithms proposed should become even more efficient than quoted in this article.

We tested the algorithms on a number of lattices varying the sizes but the conclusion we reach are valid whatever the lattices and sizes are since local algorithms are compared. Moreover we think that these improvements of the algorithms applied to spin systems are of general nature and could be applied also outside of this field.

VI. ACKNOWLEDGMENTS

We are grateful to Flavio Nogueira and Sonoe Sato for their support, discussions, and for reading the manuscript critically.

-
- [1] N. Metropolis, A.W. Rosenbluth, M.N. Rosenbluth, A.H. Teller and E. Teller, *J. Chem. Phys.* **21**, 1087 (1953).
 - [2] <http://www.physik.fu-berlin.de/~loison/>
 - [3] J.A. Plascak and D.P. Landau, *Phys. Rev. E* **67**, 015103 (2003).
 - [4] K. Hukushima and K. Nemoto, *J. Phys. Soc. Jap.* **65**, 1604 (1996), *Phys. Rev. E* **61** R1008 (2000).
 - [5] M. Creutz, *Phys. Rev. D* **36**, 515 (1987).
 - [6] B. Berg and T. Neuhaus, *Phys. Lett. B* **267**, 249 (1991), *Phys. Rev. Lett.* **68**, 9 (1992).
 - [7] D. Loison and P. Simon, *Phys. Rev. B* **61**, 6114 (2000).
 - [8] J.E. Gentle, *Random number Generation and Monte Carlo Methods*, Springer, 1998.
 - [9] W.K. Hasting, *Biometrika* **170**, 97 (1970).
 - [10] A. J. Walker, *ACM Transaction on Mathematic Software* **3**, 253 (1977).
 - [11] R. Kronmal and A. Peterson, *American Statistician*, **33**, 214 (1979).
 - [12] M. Blume, *Phys. Rev.* **141**, 517 (1966); H.W. Capel, *Physica* **32**, 966 (1966).
 - [13] e. g.: J. A. Plascak and D.P. Landau, *Phys. Rev. E* **67**, 151103 (2003);
R. da Silva, N.A Alves, and J.R.D. de Felicio, *Phys. Rev. E* **67**, 57102 (2003);
S. Grollau, *Phys. Rev. E* **65**, 56103 (2002);
M.M. Tsypin and H.W.J. Blöte, *Phys. Rev. E* **62**, 73 (2000);
S. Bekhechi and A. Benyoussef, *Phys. Rev. B* **56**, 13954 (1997).
 - [14] R.B. Potts, *Proc. Cambridge Philos. Soc.* **48**, 106 (1952).
 - [15] e. g.: Z. F. Wang, and B.W. Southern, *Phys. Rev. B* **68**, 94419 (2003); *ibid* **67**, 54415 (2003);
M. Itakura, *Phys. Rev. B* **60**, 6558 (1999);
G. Palágyi, C. Chatelain, B. Berche, et al., *Eur. Phys. J. B* **13**, 357 (2000);
M. Reuhl, P. Nielaba, and K. Binder, *Eur. Phys. J. B* **2**, 225 (1998).
 - [16] M.S.S. Challa and D.P. Landau, *Phys. Rev. B* **33** 437 (1986);

- W. Scott and H.L. Scott, J. Phys. A: Math. Gen. **22** 4463 (1989).
- [17] e. g.: J. Hove and A. Sudbo, Phys. Rev. E **68**, 46107 (2003);
A. Benyoussef, M. Loulidi, and A. Rachadi, Phys. Rev. B **67**, 094415 (2003);
N. Todoroki, Y. Ueno, and S. Miyashita, Phys. Rev. B **66**, 214405 (2002);
J. D. Noh, H. Rieger, M. Enderle, and K. Knorr, Phys. Rev. E **66**, 026111 (2002);
F. J. Resende and B. V. Costa, Phys. Rev. E **58**, 5183 (1998).
- [18] Y. Miyatake, M. Yamamoto, J.J. Kim, M. Toyonaga and O. Nagai, J. Phys. C: Solid State Phys. **19**, 2539 (1986).
- [19] E. Bayong and H. T. Diep, Phys. Rev. B **59**, 11919 (1999).
- [20] M. Hasenbusch, K. Pinn, S. Vinti, Phys. Rev. B **59** 11471 (1999) and references therein.
- [21] M. Creutz, L. Jacob, and C. Rebbi, Phys. Rep. **95**, 201 (1983).
- [22] K.J. Moriarty, Phys. Rev. D **25**, 2185 (1982).
- [23] R.G. Edwards, J. Goodman, A.D. Sokal, Nucl. Phys. B **354**, 289 (1991).
- [24] T. Hattori and H. Nakajima, Nucl. Phys. B (Proc. Suppl.) **26**, 635 (1992), J. of Comp. Phys. **121**, 238 (1995).
- [25] D. Loison, <http://www.physik.fu-berlin.de/~loison/articles/reference20.html>
- [26] S.G. Pawig, K. Pinn, Int. J. Mod. Phys. C **9**, 727 (1998).
- [27] H.G. Katzgraber and A.P. Young, Phys. Rev. B **65**, 214401 (2002).
- [28] M. Creutz, Phys. Rev. D **21**, 2308 (1980).
- [29] K. Kajantie, M. Laine, K. Rummukainen, M. Shaposhnikov, Nucl. Phys. B **466**, 189 (1996).
- [30] K. Fabricius and O. Haan, Phys. Lett. B **143**, 459 (1984).
- [31] A.D. Kennedy and B.J. Pendleton, Phys. Lett. B **156**, 393 (1985).
- [32] D. Loison, A.I. Sokolov, B. Delamotte, S.A. Antonenko, K.D. Schotte and H.T. Diep, JETP Letters **76**, 337 (2000).
- [33] D. Loison in *Frustrated spin systems*, ed. H.T. Diep, World Scientific, 2nd edit. (2004).
- [34] D. Loison, Phys. Lett. A **257**, 83 (1999); *ibid.* **264**, 208 (1999).

Figures & Figure Captions

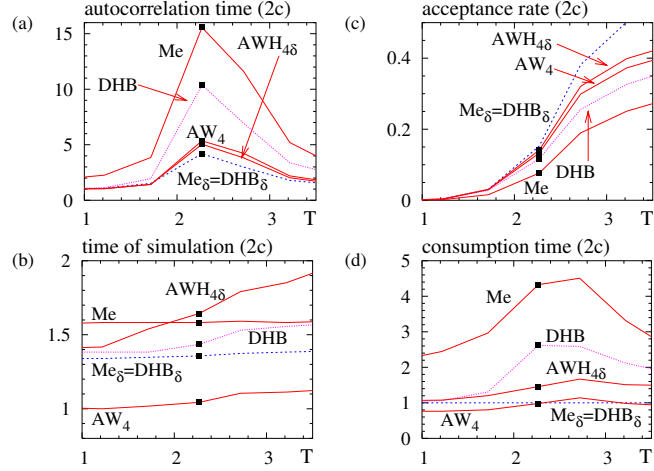


FIG. 1: Ising model. Results for a ferromagnet on a square lattice.

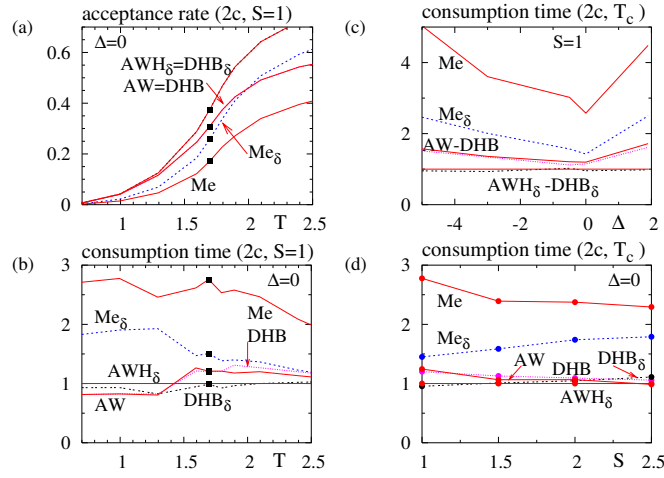


FIG. 2: Blume-Capel model on a square lattice, see text for explanations.

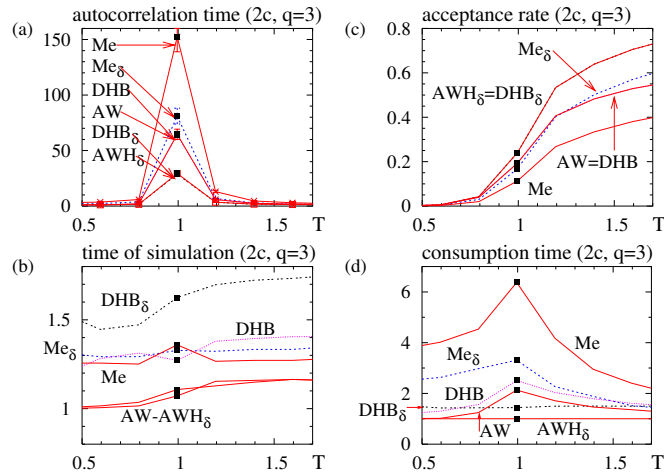


FIG. 3: Three state Potts model. Results for a ferromagnet on a square lattice.

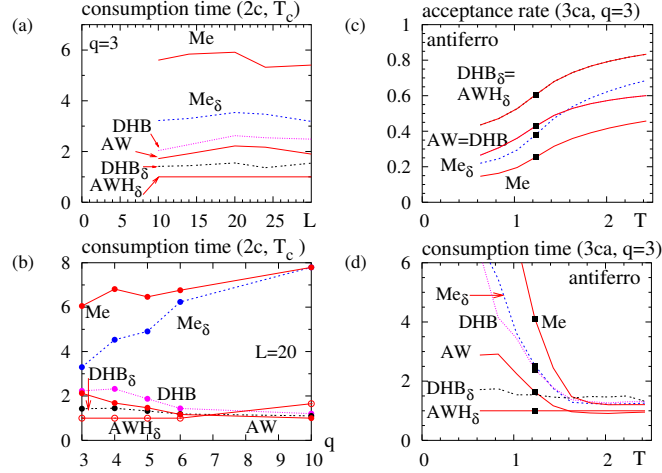


FIG. 4: q state Potts model. Results for a ferromagnet on square lattice (2s) and for an anti-ferromagnet on cubic lattice (3ca). L is the system size.

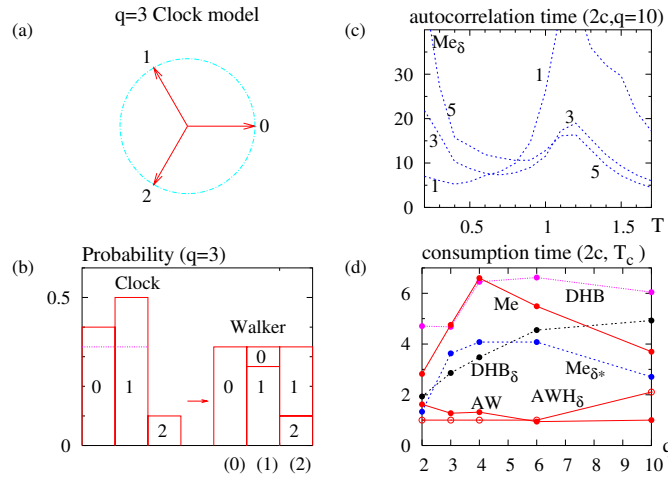


FIG. 5: q state clock model: (a) model, (b) probability and Walker's "boxes", (c) and (d) show results for a ferromagnet on a square lattice (2s).

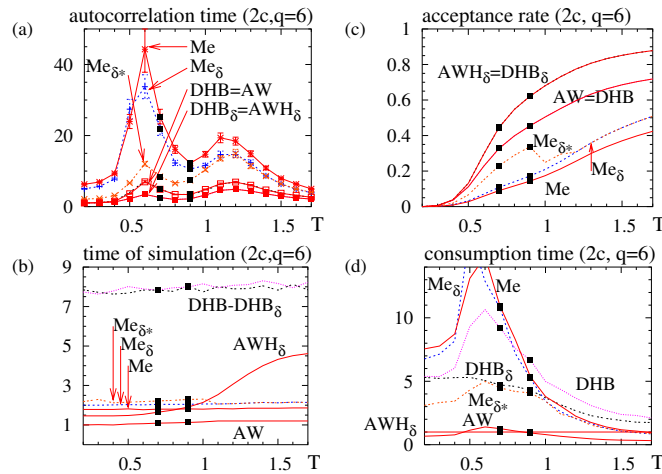


FIG. 6: $q = 6$ state clock model. Results for a ferromagnet on a square lattice.

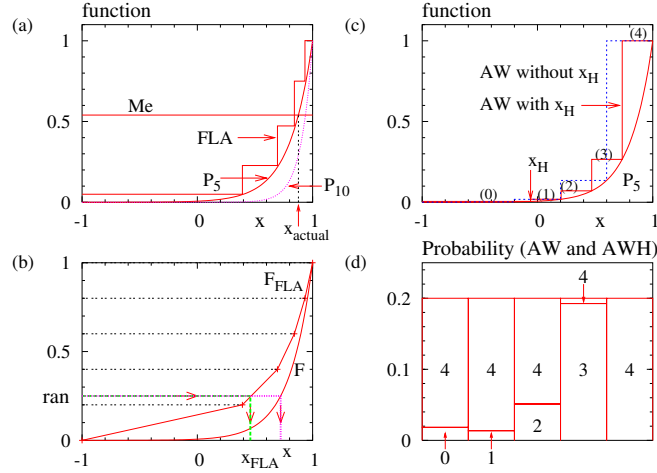


FIG. 7: Continuous Ising spin $-1 \leq S < 1$: (a) & (c) probability P and step functions f , (b) cumulative probability of P (F) and f_{FLA} (F_{FLA}) with equidistant dashed lines, (d) Walker's boxes corresponding to "AW with x_H " in (c).

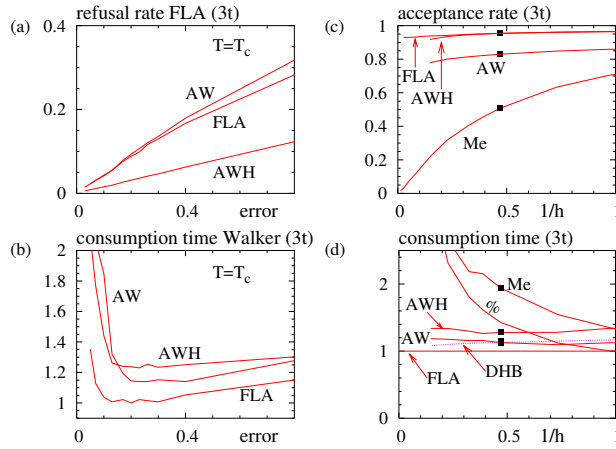


FIG. 8: Continuous Ising spin $-1 \leq S < 1$. Results for an anti-ferromagnet on a 3d stacked triangular lattice (3t), see text for explanations.

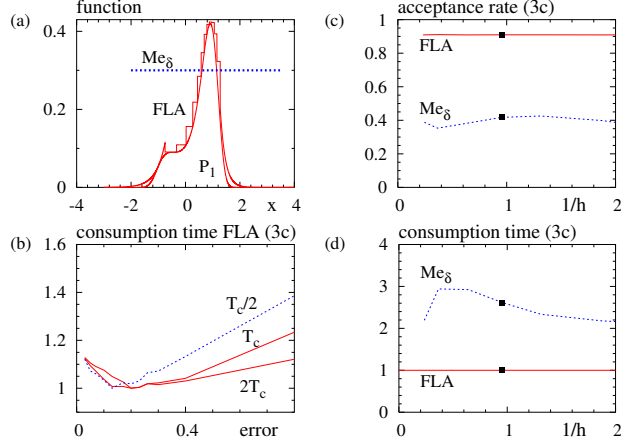


FIG. 9: Ising ϕ^4 model. (a) probability P and function f_{FLA} , (b–d) results for a ferromagnet on a cubic lattice (3c) discussed in the text.

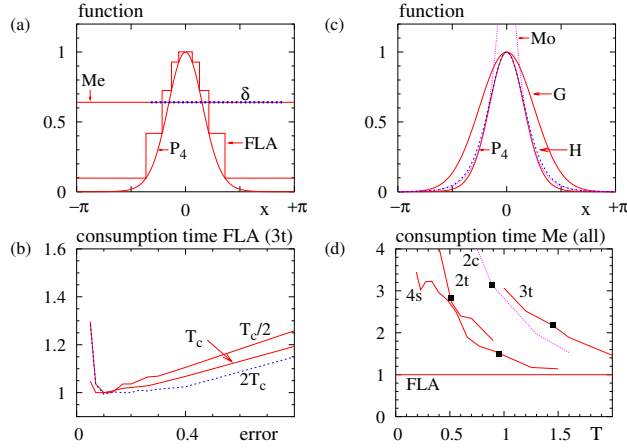


FIG. 10: XY spins. (a) & (c) probability P and functions f , consumption time (b) for FLA and (d) for Metropolis compared to FLA for different lattices.

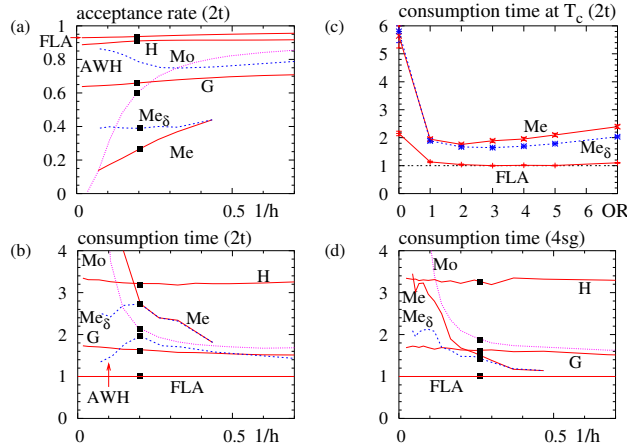


FIG. 11: XY spins. (a) & (b) results for an anti-ferromagnet on a 2d triangular lattice (2t), (c) consumption time together with over-relaxation steps OR, and (d) for a 4d spin glass (4sg) in combination with the exchange algorithm.

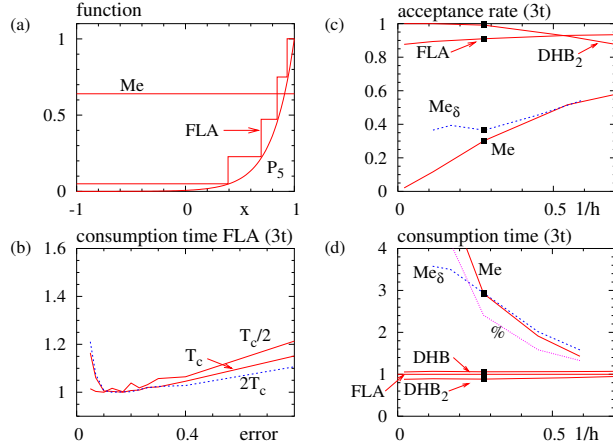


FIG. 12: Results for a Heisenberg anti-ferromagnet on a 3d triangular lattice.

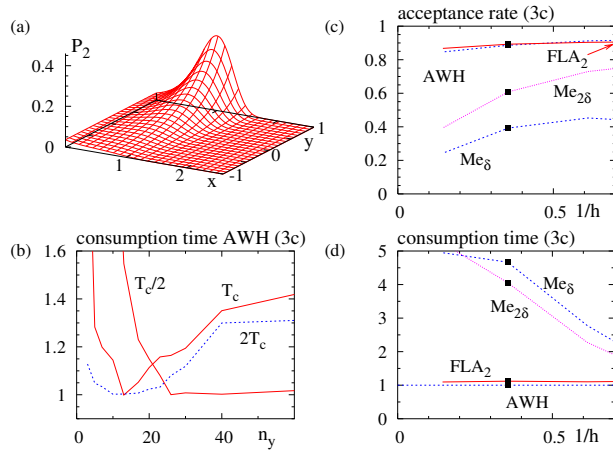


FIG. 13: Heisenberg ϕ^4 model: (a) the probability P depending on $x = \cos \theta$ and the norm y , (b-d) results for a ferromagnet on a cubic lattice.

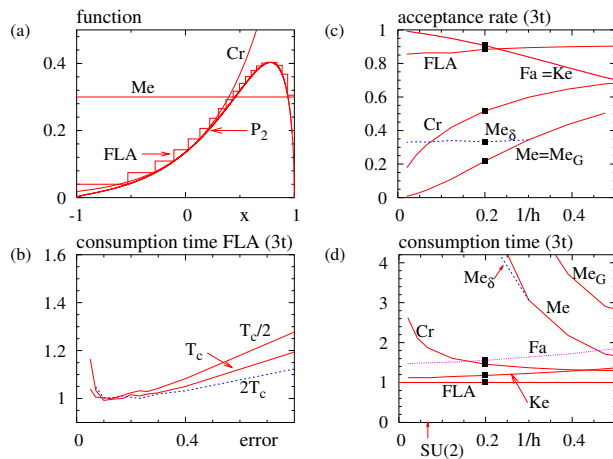


FIG. 14: Four components spins $O(4)$. Results for the 3d anti-ferromagnetic on a triangular lattice.

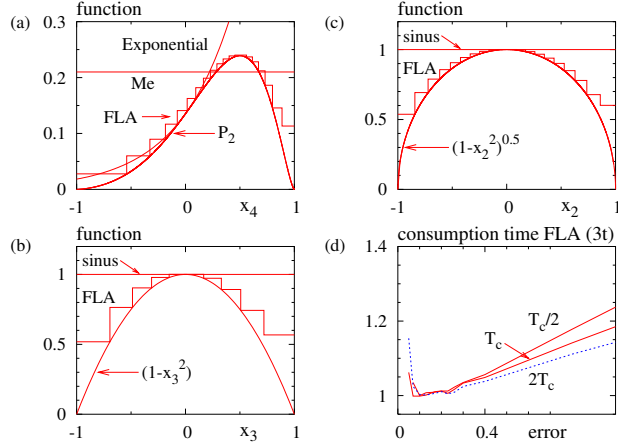


FIG. 15: Six component spins $O(6)$: (a) (b) and (c) probabilities and the corresponding step functions f . (d) Search for a minimal consumption time.

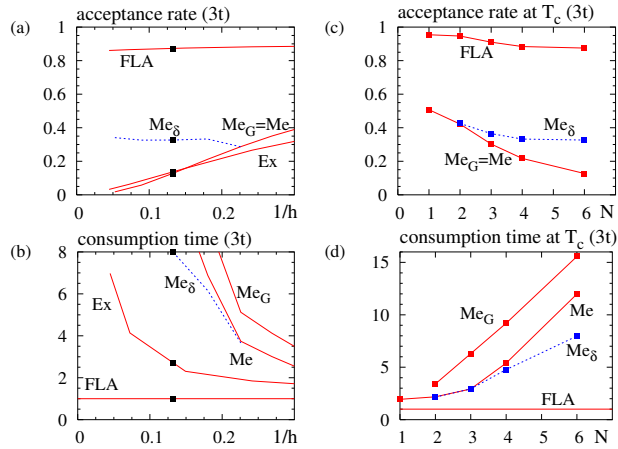


FIG. 16: N components spins. Results for an anti-ferromagnet on a 3d triangular lattice, (a) & (b) for $N = 6$. (c) & (d) for different N at T_c .